Am J Transl Res 2020;12(10):6264-6276
www.ajtr.org /ISSN:1943-8141/AJTR0111796

Original Article

IGF1- and BM-MSC-incorporating collagen-chitosan scaffolds promote wound healing and hair follicle regeneration

Ying Xia[1], Jianshe Chen[2], Juan Ding[1], Jianqing Zhang[1], Hong Chen[1]

[1]*Medical Cosmetology Department, Plastic Surgery, Shaoxing People's Hospital (Shaoxing Hospital, Zhejiang University School of Medicine), Shaoxing 312000, Zhejiang Province, P. R. China;* [2]*Department of Dermatology, The First Affiliated Hospital, Xiamen University, Xiamen 361000, Fujian Province, P. R. China*

Received April 2, 2020; Accepted August 1, 2020; Epub October 15, 2020; Published October 30, 2020

Abstract: Full-thickness skin injury affects millions of people worldwide each year. Although bone marrow-derived mesenchymal stem cells (BM-MSCs) have been shown to promote cutaneous wound healing, they cannot functionally promote wound healing with the recovery of appendages such as hair follicles. We previously found that growth factor plus BM-MSCs could effectively promote wound healing and hair follicle regeneration. In the present study, we grafted insulin-like growth factor 1 (IGF1), a multifunctional cell growth factor, and BM-MSCs into a collagen-chitosan scaffold to investigate their effects on functional wound healing. Using scanning electron microscopy, histological staining, and quantitative analysis, we found that IGF1- and BM-MSC-incorporating collagen-chitosan scaffolds promote cutaneous wound healing with effective regeneration of hair follicles in a rat full-thickness skin injury model. In addition, IGF1/BM-MSCs inhibit inflammatory cytokines during wound healing. *In vitro*, we found that IGF1 promotes the proliferation and migration of BM-MSCs via the IGFR-mediated ERK1/2 signaling pathway. Collectively, in this study, we first demonstrated that IGF1 enhances BM-MSC-mediated wound healing as well as hair follicle regeneration. Our data suggest that the topical application of IGF1 and BM-MSCs incorporated in collagen-chitosan scaffolds can be used as a feasible and effective therapeutic approach to improve functional cutaneous wound healing.

Keywords: Wound healing, hair follicle, mesenchymal stem cells, insulin-like growth factor 1

Introduction

The skin, which includes the epidermis, dermis, and appendages, is the largest organ of the human body. Due to skin defects caused by trauma, burns, and chronic diseases, nearly 10 million patients need skin grafts to repair wounds every year [1]. The skin contains hair follicles, sebaceous glands, sweat glands, and other accessory organs. Hair follicle-rich skin wounds heal faster than skin without hair follicles, and the proportion of collagen in the wound site is closer to the original normal skin after healing [2]. Therefore, therapeutic approaches targeting hair follicle regeneration may be an effective method to promote wound healing after trauma.

Mesenchymal stem cells (MSCs) are bone marrow-derived non-hematopoietic progenitor cells [3]. MSCs have been shown to enhance cutaneous wound healing. Transplanting MSCs into severe burn wounds with full cortical defects can effectively promote thickening of the epidermal tissue, increase the relative number of nerve fibers in the dermis, and shorten the skin repair cycle [4]. MSCs can also reduce wound inflammation, promote angiogenesis, regulate ECM synthesis, and promote skin structural regeneration and functional recovery to a certain extent [5]. These results suggest that MSCs have great application prospects in skin repair. Although MSCs can promote wound skin repair, the performance of MSCs alone in wound hair follicle regeneration is unsatisfactory [6]. Improving the microenvironment, maintaining the cell activity, and promoting the proliferation, migration, and differentiation of MSCs is the key to the clinical application of MSCs in wound healing [7].

Insulin-like growth factor 1 (IGF1), a multifunctional cell growth factor, regulates cell proliferation, migration, and epithelialization [8]. Low expression of IGF1 was observed in the ulcerative wound skin of diabetic patients [9]. Treating a rat acute wound model with IGF1-overexpressing fibroblasts significantly enhanced wound healing speed [10]. In the process of artificially inducing MSCs to differentiate into fibroblast cell lines, researchers have observed that IGF1 participates in the regulation of fibroblast proliferation, migration, and collagen synthesis [11]. The study also found that the IGF1-mediated signaling pathway might play an important regulatory role in hair growth and decay [12]. These findings indicate that IGF1 may serve as a regulator of hair follicle regeneration. However, the role of IGF1 in wound healing is unknown.

The collagen-chitosan scaffold has good biocompatibility, low antigenicity, and high biodegradability [13]. There are a large number of space voids in this three-dimensional structure, which is suitable for cell adhesion and proliferation, and is conducive to the exchange of liquid inside and outside [14]. Bone marrow-MSCs grafted with collagen-chitosan scaffolds have been shown to accelerate the healing of severe burn wounds [15]. Our previous study has also identified that using a collagen-chitosan scaffold, epidermal growth factor, and MSCs not only promotes wound healing in rats after trauma, but also hair follicle regeneration [16]. Therefore, in the present study, we loaded IGF1 and BM-MSCs onto a collagen-chitosan scaffold and determined the role of IGF1/BM-MSCs in the repair of large-area full-thickness skin defects and the regeneration of hair follicles. In addition because MSC activity is a key factor for the promotion of wound healing [17], we further investigated whether IGF1 promoted the proliferation and migration of BM-MSCs and the potential underlying mechanisms.

Materials and methods

Ethics statement

The animal protocol and experimental procedures were approved by the Institution of Animal Care and Use Committee of Shaoxing People's Hospital.

Preparation, isolation, identification, and labeling of BM-MSCs in culture

We performed the isolation of rat BM-MSCs as described in our previous study [16]. In brief, bone marrow cells were flushed from the tibias of adult male SD rats with PBS. Flushed cells (15 ml) were centrifuged at 1000 × g for 5 min. The supernatant was removed, and cells were washed with RPMI-1640 medium and centrifuged for an additional 5 min. Finally, the cells were resuspended in medium containing 10% fetal bovine serum (FBS, Gibco) and 1% penicillin/streptomycin (Beyotime, Jiangsu, China) in 25-mL culture flasks and incubated at 37°C in a fully humidified atmosphere with 5% CO_2. Cells were characterized using fluorescence-activated cell sorting (FACS) to assess the positivity of a cluster of differentiation CD31, CD44, CD73, CD90, and CD105. Besides, BM-MSCs were identified by detecting osteogenic and adipogenic differentiation. Osteogenic differentiation was visualized by staining with Alizarin Red staining, and adipogenic differentiation was visualized using Oil-Red-O staining. The labeling of BM-MSCs was performed as described previously. According to the manufacturer's protocol, BM-MSCs were labeled with CM-DiI (1, 1'-dioctadecyl-3,3,3',3'-tetramethylindocarbocyanine perchlorate, Beyotime) and cultured in the dark at 37°C for 30 min. BM-MSCs were then washed with PBS and centrifuged at 1000 × g for 5 min. Images were acquired using a Leica DFC3000 fluorescence microscope.

Preparation of collagen-chitosan scaffolds

Collagen and chitosan were dissolved in 0.5 M acetic acid to form a 0.5% (w/v) solution at a mass ratio of 9:1. The collagen-chitosan composite was injected into homemade molds, frozen at -20°C for 2 h, and lyophilized for 24 h to produce a porous collagen-chitosan scaffold (2 cm × 2 cm × 0.5 cm). After disinfection in 75% alcohol, BM-MSC scaffolds were cultured with CM-DiI-labeled BM-MSCs at a cell concentration of 5 × 10^6/μL at 37°C in a 5% CO_2 atmosphere. IGF/BM-MSC scaffolds were cultured with labeled BMSCs and 100 nM IGF1 (SRP0350, Sigma). Each scaffold was kept in a saturated humidity incubator for 48 h, and the morphology of adhered cells within scaffolds was observed by scanning electron

microscopy (SEM, SU-70, Hitachi, Hangzhou, China).

Rat cutaneous wounds and treatment

The rat cutaneous wound was constructed as described in our previous study [16]. Briefly, rats were anesthetized with 3% pentobarbital sodium solution (Sigma) via intraperitoneal injection. Three full-thickness wounds with a diameter of 2.0 cm were established on the backs of the rats using a round biopsy punch. A total of 18 rats (approximately 10 weeks old, 250±20 g) were used for the experiments. The wounds were randomly divided into three groups: Control, BM-MSCs, and IGF1/BM-MSCs groups. The blank, BM-MSCs, and IGF1/BM-MSCs scaffolds were then extended on the wound bed and sutured to the adjacent skin. Petrolatum gauze was used to cover the wounds and was removed seven days later. Rats were killed in batches of 6 on days 7, 21, and 35 post-surgery.

Wound closure and hair follicle regeneration analysis

A measuring ruler was used to measure the wound size. After image capture, wound closure was quantified (mm^2) on days 7, 21, and 35 post-surgery using ImageJ software. The wound closure rate was calculated as the percentage of the wound area on day X compared with the wound area on postoperative day 0. For hair follicle regeneration analysis, the number of new hair follicles on day 35 was determined by counting 6 randomly selected image areas according to the versican staining.

Pathological staining

The obtained wound tissues were fixed in 10% formalin, decalcified, dehydrated, cleared with dimethylbenzene, and embedded in paraffin. Five-micrometer sections were stained with hematoxylin and eosin (H&E) and Oil Red staining according to the manufacturer's instructions. For immunohistochemistry, the slides were treated with primary antibody against versican overnight at 4°C. Following incubation with the primary antibody, the slides were blocked for 1 h at 37°C and washed with PBS. The secondary antibody was reacted with the slides for 30 min. After washing with PBS, the slides were treated with DAB (Solarbio, Beijing, China) to visualize the immunoreactivity. Images were obtained using a Leica DM3000 microscope (Leica Company, Germany).

Measurement of inflammatory cytokines

The wound tissue was lysed with protein lysis buffer. ELISA kits (Nanjing SenBeiJia Bio-Technology Co., Nanjing, China) were used to detect the levels of tumor necrosis factor α (TNF-α), interferon-γ (IFN-γ), interleukin 1β (IL-1β), and interleukin 6 (IL-6) in tissue homogenates by following the manufacturer's protocol.

Real-time quantitative PCR

Total RNA from BM-MSCs was extracted using TRIzol kits (Takara, Japan). The cDNA was obtained using a PrimeScript RT reagent kit (Takara). Then, real-time PCR was performed using SYBR premix Ex Taq reagent kit (Takara) through the 7500 real-time PCR system (Applied Biosystems, USA) according to the manufacturer's instructions. The mRNA levels were normalized against GAPDH levels and the expressions of target genes were calculated using the $2^{-\Delta\Delta Ct}$ method. The following PCR primers were used: IGF1, forward: 5'-TTCAACAAGCCCACAGGGTA-3', reverse: 5'-GCAATACATCTCCAGCCTCCT-3'; GAPDH, forward: 5'-TGCACCACCAACTGCTTAGC-3', reverse: 5'-GGCATGGACTGTGGTCATGAG-3'.

Western blot

Total protein from hippocampal neuronal cells was obtained by adding RIPA buffer (Beyotime) containing phosphatase inhibitor (MedChemExpress, Shanghai, China). The protein concentration was measured with a BCA Protein Quantification Kit (Beyotime). A total of 30 μg protein was separated on 12% SDS-PAGE and transferred onto PVDF members. The members were blocked by 5% non-fat milk for 30 min and incubated with the following antibodies against IGF1R (ab39675, Abcam), p38 (lot:8690, CST), p-p38 (lot:4511, CST), ERK1/2 (lot:4695, CST), p-ERK1/2 (lot:4370, CST), JNK (lot:9252, CST), p-JNK (lot:4668, CST) and β-actin (ab8226, Abcam) at 4°C overnight. The membrane was further incubated for 1 h with horseradish peroxidase (HRP)-labeled secondary goat anti-rabbit antibody (Beyotime). The membranes were treated with

an enhanced chemiluminescent detection kit (Beyotime), and the signals were photographed on a gel imaging system (Bio-Rad Laboratories, Inc., Hercules, CA, USA). The relative expression of the proteins was expressed as the gray value ratio between the band of protein to be assessed relative to that of β-actin.

MTT assay

Cell proliferation of cells was detected by MTT assay. At the end of the treatment for various time (1, 2, 3, 4 and 5 days), MTT solution (5 mg/ml) was added to each well and incubated for another 4 h. Then the medium was removed and 100 μL DMSO was added to dissolve formazan. Finally, a SpectraMax Plus Absorbance microplate reader (Molecular devices, CA, USA) was used to measure the absorbance at 570 nm.

Wound healing assay

A wound healing assay was performed to evaluate the cell migrative ability. When BM-MSCs reached 90% confluence, a micropipette tip was taken to make a scratch across the surface. PBS was used to wash the suspended cells, and FBS-free DMEM was added. After 24 h, images of cells were taken by a light microscope (Nikon Corporation, Tokyo, Japan).

Statistical analysis

Grouped data are expressed as the mean ± SD. Student's t test was used for two-group comparisons and multiple group comparisons were achieved using one-way ANOVA analysis, followed by Bonferroni post-hoc tests. All statistical analyses were conducted using GraphPad Prism 7.0 (GraphPad Prism, Inc., La Jolla, CA, USA). Differences of $P < 0.05$ were considered statistically significant.

Results

Isolation and identification of BM-MSCs

A homogenous population of BM-MSCs was obtained after 3 passages. Flow cytometry assays showed that these fibroblast-like cells expressed surface markers of mesenchymal stem cells. They were positive for CD73, CD44, CD90, and CD105, but negative for CD31 (**Figure 1A**). Under adipogenic and osteogenic culture conditions, BM-MSCs were capable of differentiating into adipocytes and osteoblasts, respectively, as evidenced by the presence of intracellular lipid droplets (Oil red O staining) (**Figure 1B**) and calcium nodule formation (ALP staining) (**Figure 1C**). These results indicated that we had efficiently generated BM-MSCs, which were used in the following experiments.

IGF1/BM-MSCs promote wound healing and hair follicle regeneration in vivo

The present study used a collagen-chitosan scaffold as a carrier for BM-MSCs and recombinant IGF1. SEM observation of the scaffolds showed a continuous structure of irregular interconnected pores. Upon the addition of BM-MSCs, the surface morphology became rough (**Figure 2A**). To further confirm the adherence of surviving cells, CM-Dil was used to mark BM-MSCs, and SEM showed the cross-linking of chitosan and BM-MSCs (**Figure 2B**). As shown in **Figure 2C**, the skin wound healing effect of the BM-MSC group was better than that of the control group, and the effect of the IGF1/BM-MSC group was better than that of the BM-MSC group. The statistical analysis showed that the residual wound area ratio of the IGF1/BM-MSC group was significantly smaller than that of the BM-MSC and the control group both 21 and 35 days after trauma. Moreover, histological analysis, including H&E staining of skin sections, showed that BM-MSCs and IGF1/BM-MSCs accelerated the return of the structural layers of the skin (**Figure 3A**). Oil red staining demonstrated that wounds treated with BM-MSCs or IGF1/BM-MSCs not only developed anatomical features (epidermal, dermal layers, and hypodermal layers) of the skin, but also healed with hair follicles by day 35 (**Figure 3B**). To precisely evaluate the hair follicle regeneration effect of IGF1/BM-MSCs, IHC with versican antibody staining was performed. The results in **Figure 3C** show that BM-MSCs promoted hair follicle regeneration and that the number of hair follicles on day 35 was significantly increased in the IGF1/BM-MSC group compared to the BM-MSC group (**Figure 3D**). Collectively, these results indicate that IGF1/BM-MSCs promote wound healing and hair follicle regeneration in mice after trauma.

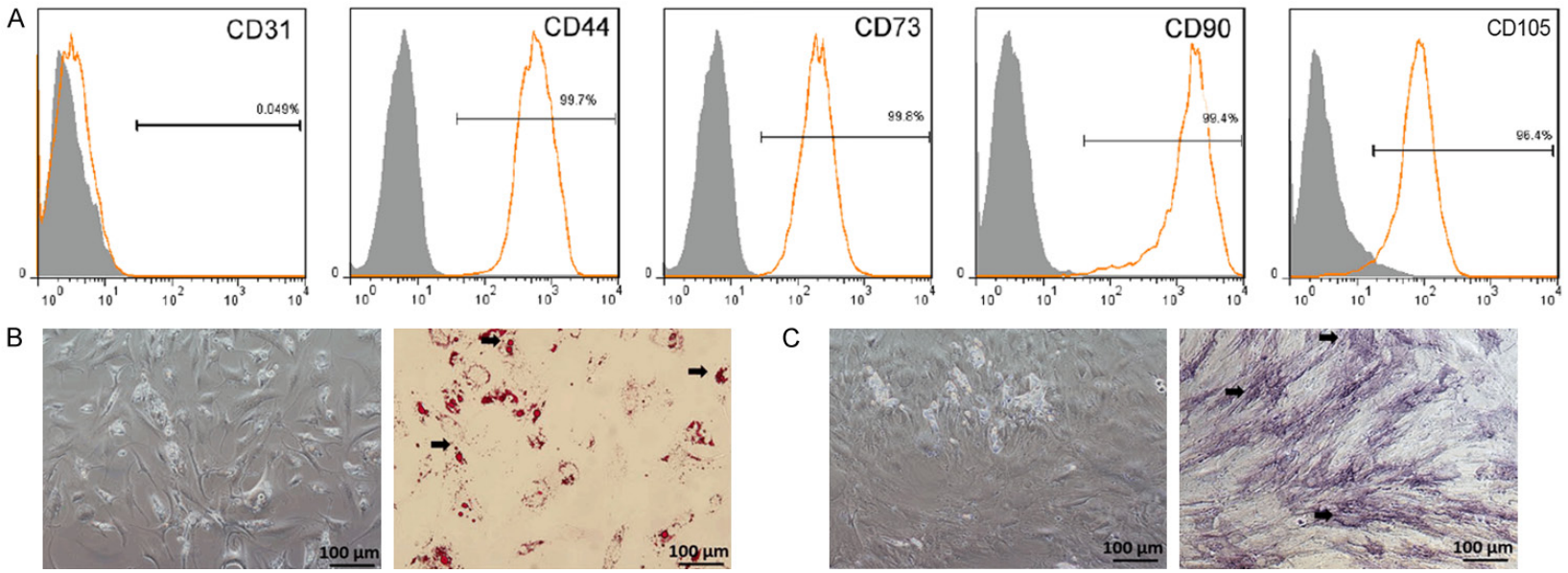

Figure 1. Isolation and characterization of BM-MSCs. A. Flow cytometry assays were used to measure the expression of cell surface markers on isolated BM-MSCs and the isolated cells were positive for CD44, CD73, CD90, and CD105, but negative for CD31. B. After culturing under adipogenic conditions, Oil Red O staining was used to evaluate adipogenesis. C. After culturing under osteogenic conditions, ALP staining was used to evaluate osteogenesis.

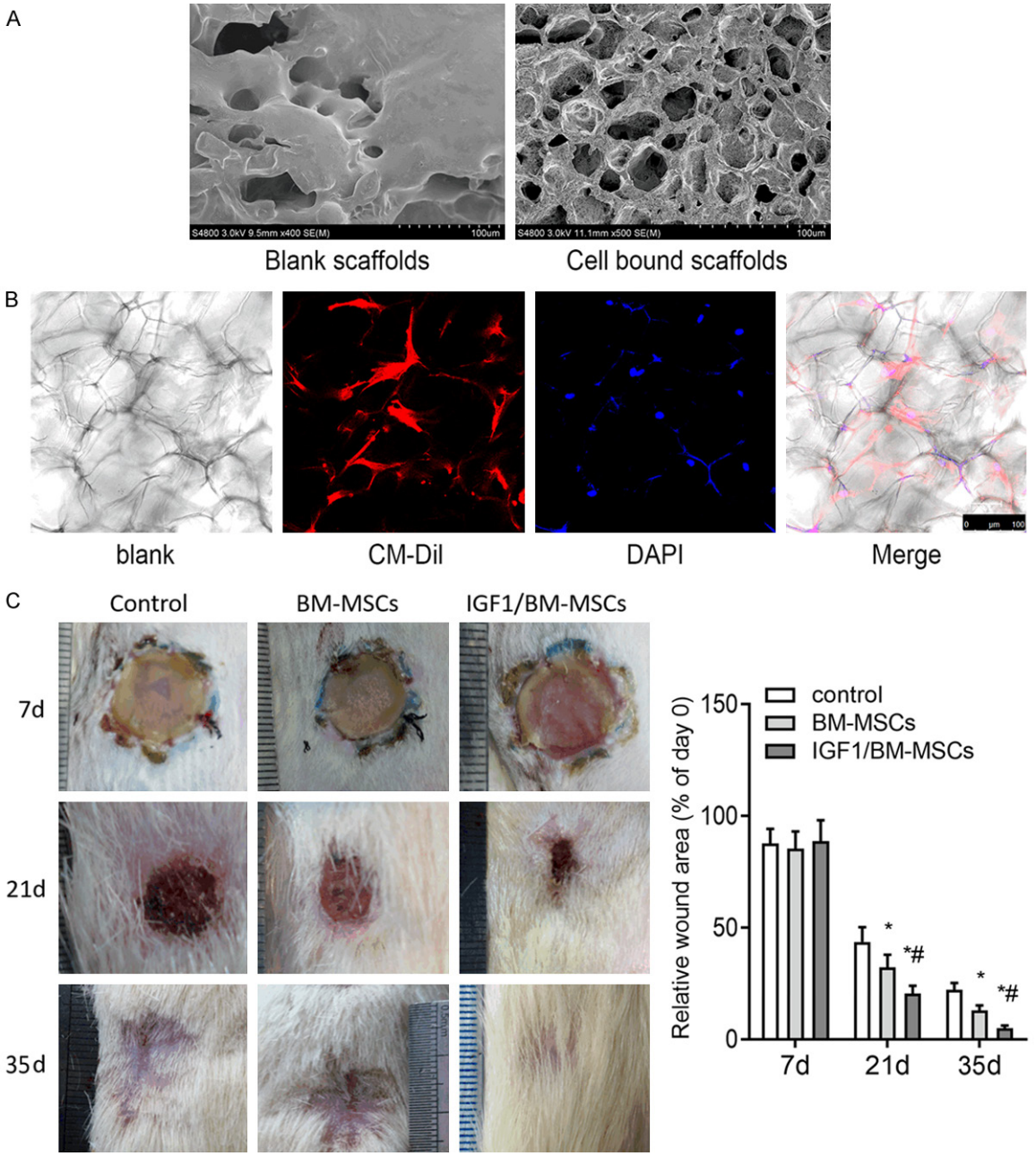

Figure 2. IGF1/BM-MSCs promoted wound healing *in vivo*. A. SEM micrographs of the surface morphology of BM-MSC-incorporating collagen-chitosan scaffolds. B. BM-MSCs were stained with CM-Dil (red) and DAPI (blue), and the BM-MSCs incorporated into the collagen-chitosan scaffold were observed under a fluorescence microscope. C. Images of the cutaneous wounds in rats showed that the skin wound healing effect of the IGF1/BM-MSCs group was better than those of the control and BM-MSCs groups 21 and 35 days after trauma. Statistical analysis showed that the area of cutaneous wounds in the IGF1/BM-MSCs group was smaller than those in the control and BM-MSCs groups 21 and 35 days after trauma. *P < 0.05 vs. control group; #P < 0.05 vs. BM-MSC group.

IGF1/BM-MSCs inhibited inflammation in skin wounds

The inflammatory response to skin wounds involves a variety of cytokines, including TNF-α, INF-γ, IL-1β, and IL-6. ELISA was used to detect the expression of these cytokines in skin wounds. **Figure 4A-D** shows the expression of the above four proinflammatory cytokines in the skin wounds of the control, BM-MSC, and IGF1/BM-MSC groups on days 7, 21, and 35 after trauma. At each time point, the expres-

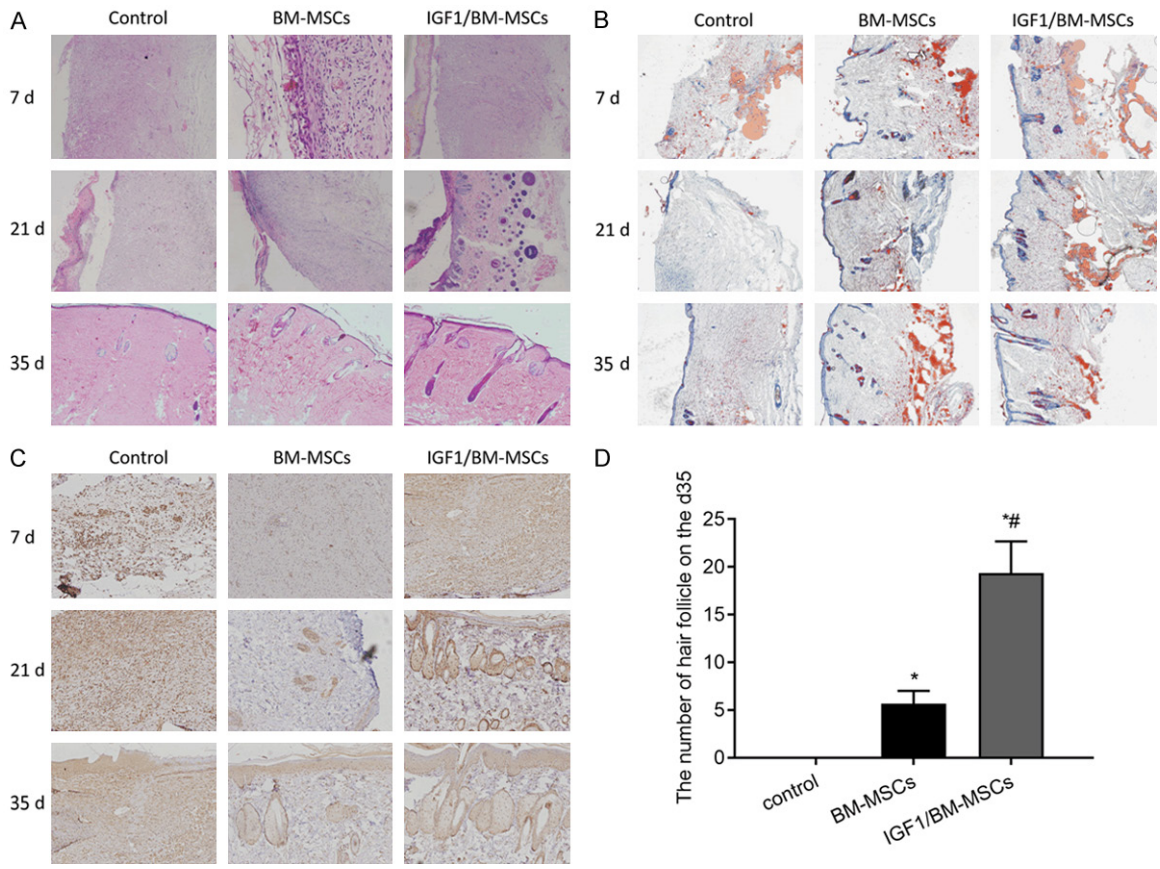

Figure 3. IGF1/BM-MSCs promoted hair follicle regeneration *in vivo* H&E (A) and Oil red O staining (B) of the wounds treated with blank scaffold (control), BM-MSC-incorporating scaffold (BM-MSCs), and scaffold containing BM-MSCs and IGF1 for 7, 21, and 35 days post trauma. The wound-healing effect of IGF/BM-MSC was better than BM-MSCs. (C) Detection of Versican expression in skin wounds in rats by immunohistochemistry in the control, BM-MSC, and IGF1/BM-MSC groups 7, 21, and 35 days after trauma. (D) Quantitative analysis of the number of hair follicles in the cutaneous wound on the 35th day according to the Versican staining. IGF/BM-MSC showed the better promoting effects than BM-MSCs on hair follicle regeneration. *P < 0.05 vs. control; #P < 0.05 vs. BM-MSCs.

sion levels of TNF-α, INF-γ, IL-1β, and IL-6 in the BM-MSC group were significantly lower than those in the control group. On days 7 and 21 after trauma, the expression levels of the four cytokines were significantly lower in the IGF1/BM-MSC group than in the BM-MSC groups. However, on day 35 there was no statistical difference between the BM-MSC and the IGF1/BM-MSC groups.

IGF1 promotes the proliferation and migration of BM-MSCs via the IGF1R pathway

To investigate the role and mechanism of IGF1 on the cell proliferation and migration of BM-MSCs, we first performed an MTT assay. As shown in **Figure 5A**, IGF1 (1, 10, and 100 nM) promoted the proliferation of BM-MSCs in a dose-dependent manner. Meanwhile, the wound-healing assay showed that IGF1 enhanced the migration ability of BM-MSCs in a dose-dependent manner (**Figure 5B** and **5C**). Since IGF1 always exerts its role via the IGF1 receptor (IGF1R) [18], we next determined the influence of IGF1 on IGF1R expression in BM-MSCs. The results showed that 100 nM IGF1 increased the protein expression of IGF1R in a time-dependent manner (**Figure 5D**).

ERK1/2 signaling mediates IGF1-induced BM-MSC proliferation and migration

Given the role of MAPK signaling in the proliferation of MSCs [19], we investigated whether this signaling pathway also participated in the IGF1-mediated proliferation of MSCs. As illustrated in **Figure 6**, 100 nM IGF1 in BM-MSCs significantly increased the protein expression

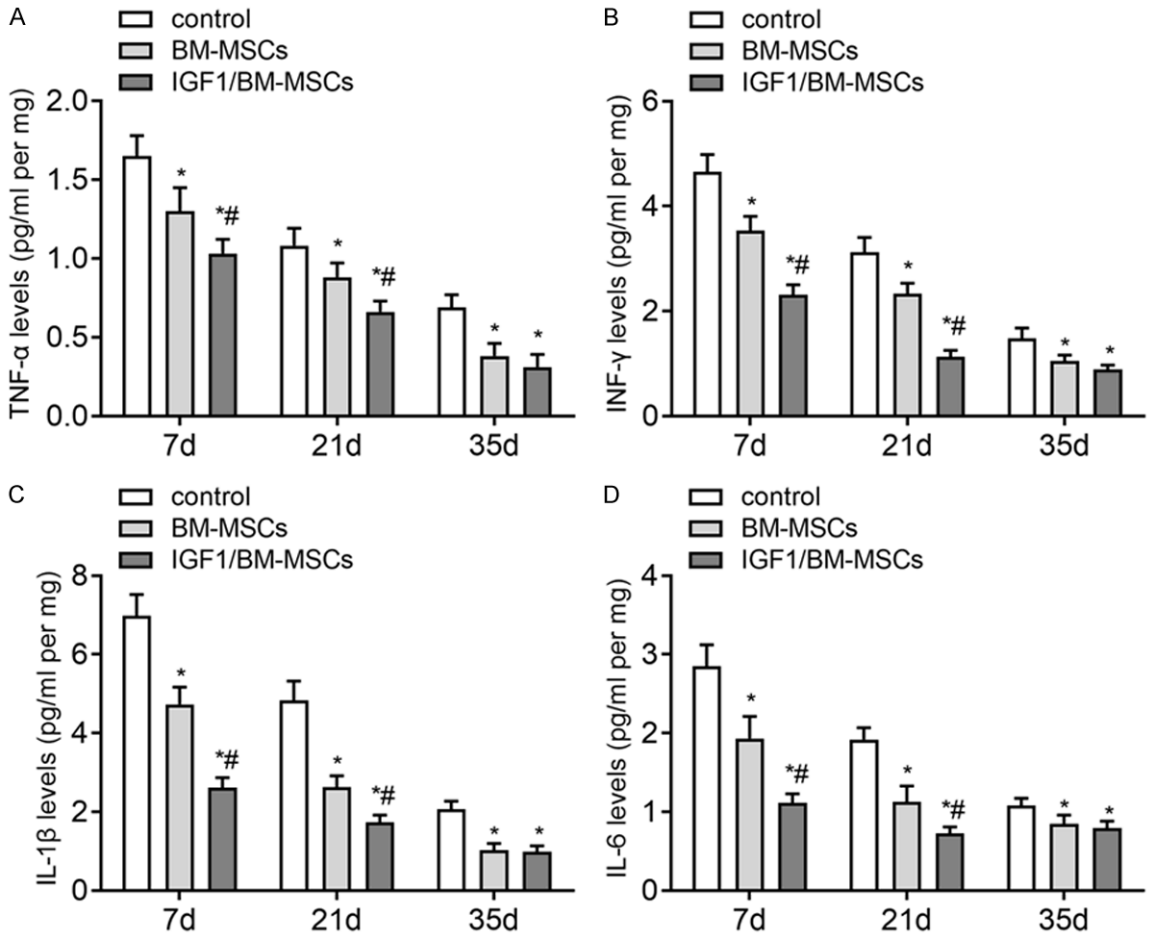

Figure 4. IGF1 and BM-MSC-incorporating collagen-chitosan scaffolds inhibited the expression of inflammatory cytokines, including TNF-α (A), INF-γ (B), IL-1β (C), and IL-6 (D), as shown by ELISA assays in the control, BM-MSC, and IGF1/BM-MSC groups 7, 21, and 35 days after trauma in the wounded skin of rats. *P < 0.05 vs. control; #P < 0.05 vs. BM-MSCs.

of p-p38 and p-pERK1/2, but not p-JNK, suggesting a cooperative effect between IGF1 and MAPK signaling. Thereafter, p38 and ERK1/2 signaling was abolished by treatment with SB203580 and U0126, respectively, as evidenced by western blot analysis (**Figure 7A**). The results of the MTT assay showed that the addition of U0126 blocked IGF1-mediated proliferation (**Figure 7B**) and migration (**Figure 7C**). However, treatment with SB203580 had no influence on the IGF1-mediated proliferation and migration of BM-MSCs. Taken together, these data indicate that IGF1 may promote proliferation and migration via the ERK1/2 signaling pathway.

Discussion

Hair follicles are an important part of the skin. In full-thickness wounds, the ability to regenerate hair follicles is reduced or even completely lost. Although great improvements have been made in the treatment of acute skin defects, the regeneration of functional skin appendages, such as hair follicles, is still challenging [20]. Therefore, the development of biomaterials that promote the regeneration of burned skin and hair follicles has huge clinical significance. The ideal wound dressing should be designed to have excellent biocompatibility, good mechanical properties as barriers, the ability to create a native extracellular matrix to stimulate cell migration, and the ability to promote tissue structure proliferation and recombination [21]. In our study, SEM micrographs showed the interconnected porous structures of collagen-chitosan and BM-MSCs loaded with collagen-chitosan scaffolds, and the spongy structure of the scaffolds facilitated the exchange of nutrients and fluids during wound

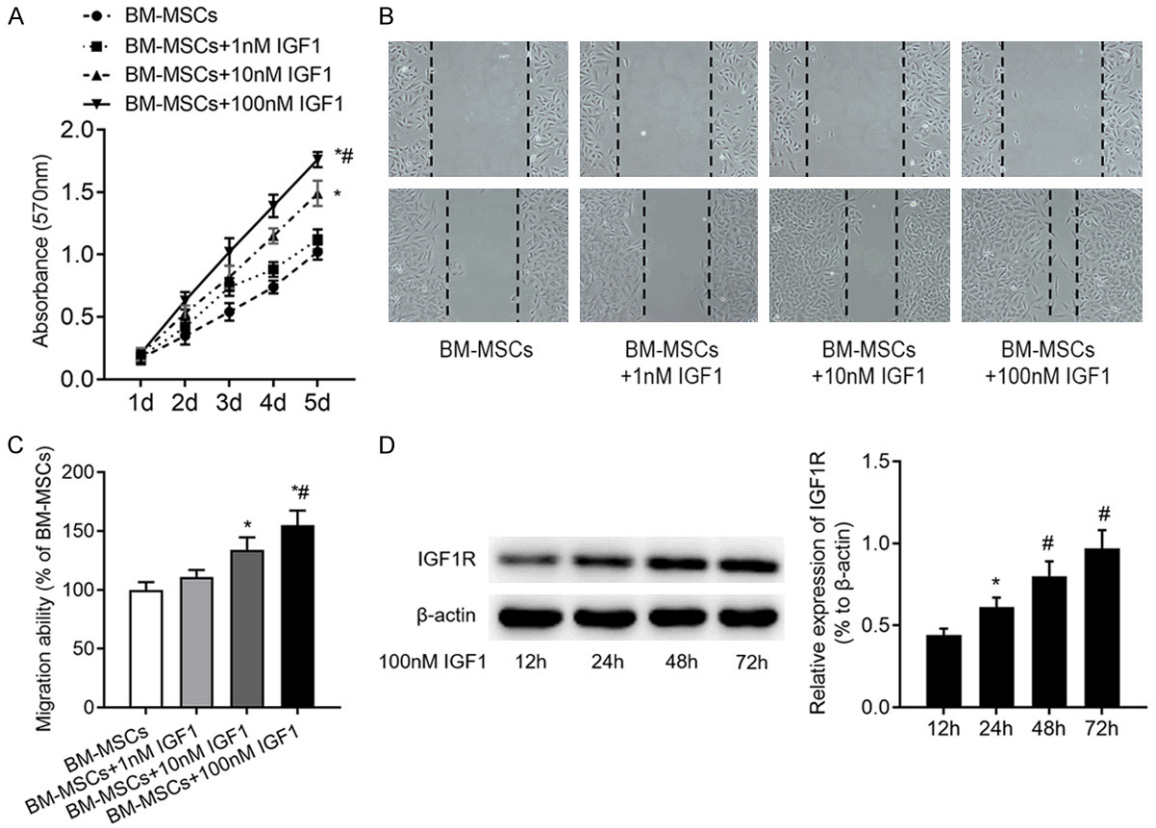

Figure 5. IGF1 promoted the proliferation and migration of BM-MSCs via the IGF1R pathway. A. The results of MTT assays showed that IGF1 promoted the proliferation of BM-MSCs in a concentration-dependent manner. B, C. Wound-healing assays showed that IGF1 enhanced the migrative ability of BM-MSCs in a concentration-dependent manner. D. Western blot analysis revealed that 100 nM IGF1 increased the levels of phosphorylated IGFR in BM-MSCs in a time-dependent manner. *P < 0.05 vs. BM-MSCs; #P < 0.05 vs. BM-MSCs+1 nM IGF1.

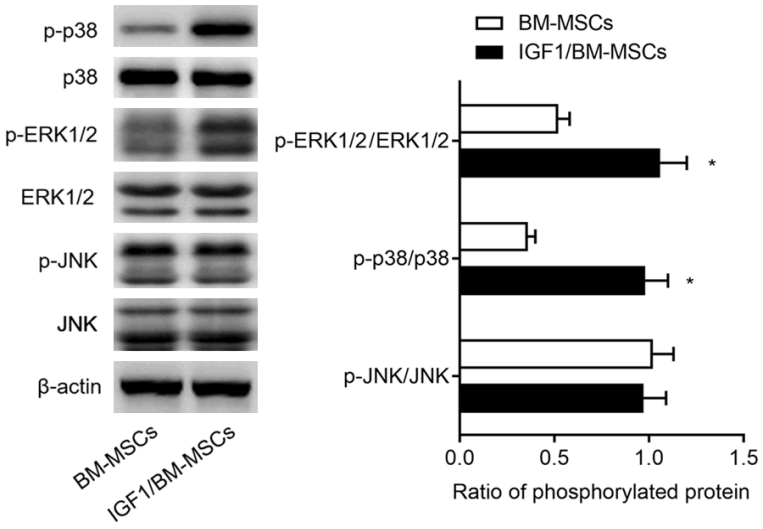

Figure 6. Western blot analysis showed the expression of phosphorylated p38, ERK1/2, and JNK in BM-MSCs treated with 100 nM IGF1 for 48 h. Phosphorylation levels of p38, ERK1/2, and JNK were quantified by densitometry and normalized to total kinase expression in the above groups. *P < 0.05 vs. BM-MSCs.

healing [22]. Consistent with a previous study [23], the isolated BM-MSCs in this study expressed typical MSC surface markers such as CD44, CD73, and CD90, and have the potential to differentiate into mesenchymal cells, including adipocytes and osteocytes. Many studies, including our previous study [16], have successfully used BM-MSCs to promote cutaneous wound healing [24]. Consistent with previous studies [25, 26], we found that although MSCs have been approved to serve as a therapeutic tool in wound healing, they have little effect on hair follicle regeneration. Functi-

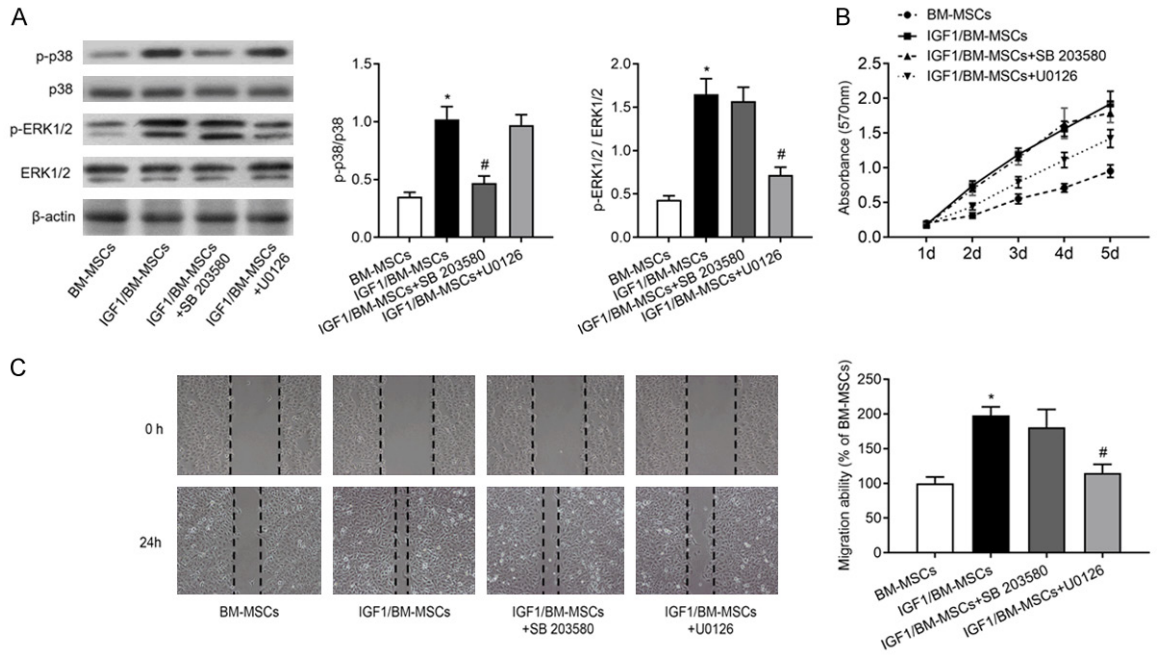

Figure 7. ERK1/2 signaling mediated the positive effects of IGF1 on the proliferation and migration of BM-MSCs. A. Western blots and quantitative analysis of phosphorylated p38 and ERK1/2 in BM-MSCs treated with 100 nM IGF1, with or without the p38 inhibitor SB 203580 and the ERK1/2 inhibitor U0126. B. MTT assays showed that U0126, but not SB 203580, reversed the effects of IGF1 on the proliferation of BM-MSCs. C. Wound-healing assays demonstrated that U0126, but not SB 203580, reversed the effects of IGF1 on the migration of BM-MSCs. *P < 0.05 vs. control; #P < 0.05 vs. IGF1/BM-MSCs.

onal regeneration of hair follicles is thus still a great challenge.

Growth factors such as fibroblast growth factor, epidermal growth factor, and the platelet-derived growth factor have received significant attention in the field of wound healing in the past few decades [7, 27, 28]. Bio-inspired hydrogels with fibroblast growth factors can enhance cell proliferation, wound re-epithelialization, and collagen deposition without any noticeable toxicity and inflammation compared to blank hydrogels and commercial wound healing products [29]. In our previous study, the results suggested that the epidermal growth factor significantly enhanced BM-MSC-mediated wound healing as well as hair follicle regeneration [16]. In this study, we observed that the topical application of an IGF1/BM-MSC-incorporating scaffold also promoted cutaneous wound healing and hair follicle regeneration. Our results were supported by the important role of IGF1 in skin development and homeostasis [12]. The exact mechanisms underlying the hair follicle-regenerative properties of IGF1 still need to be identified. In addition, we found that compared to the BM-MSC group, treatment with IGF1 and BM-MSCs caused a further decrease in several inflammatory cytokines including TNF-α, INF-γ, IL-1β, and IL-6, which are thought to be involved in vascular proliferation and immune regulation during skin wound healing [30]. The effects of IGF1 on inflammatory cytokines may be due to its effect on the secretion role of BM-MSCs.

The proliferation and migration of BM-MSCs in the wound are important during wound healing processes [31]. Therefore, we investigated the effects of IGF1 on BM-MSCs *in vitro*, as well as its potential mechanism. IGF1 promotes the proliferation of various cell types, including epithelial cells, muscle cells, and some stem cells [32]. A recent study found that IGF1 enhanced BM-MSC viability, migration, and anti-apoptosis via the secreted frizzled-related protein 2 pathway [33]. Here, we showed that IGF1 upregulated IGF1R in BM-MSCs and that 1-100 nM IGF1 facilitated the proliferation and migration of BM-MSCs. Expression of IGF1R and activation of IGF1/IGF1R down-

stream signaling is important for regulating tissue homeostasis in stromal wound healing [34]. MAPK signaling is a key player in cell migration, angiogenesis, and tissue development [35]. Our experiments demonstrated that IGF1 induced the phosphorylation of ERK1/2 and p38 but had no influence on the phosphorylation of JNK in BM-MSCs. Consistent with our results, IGF1 was found to activate the MAPK/ERK1/2 signaling pathway to promote cell proliferation in osteoblasts [36]. Furthermore, we found that inhibition of ERK1/2 signaling effectively abrogated IFG1-mediated BM-MSC proliferation and migration. In contrast, inhibition of p38 signaling had no substantial effects on BM-MSC proliferation. In conclusion, our results indicate that IGF1 induces the proliferation and migration of BM-MSCs through IGFR-mediated activation of the ERK1/2 signaling pathway, but not through p38 signaling. In contrast, MSC therapies for wound healing are also effective due to the transdifferentiation of MSCs into different cell lineages, such as endothelial-like cells and keratinocytes [37]. Whether IGF1 can facilitate the differentiation of BM-MSCs still needs to be investigated in future studies.

Conclusion

In summary, we found that IGF1/BM-MSCs promoted cutaneous wound healing and hair follicle regeneration in rats. IGF1 promoted the proliferation and migration of BM-MSCs via the IGFR-mediated ERK1/2 signaling pathway. These findings demonstrate a potential new approach to synergistically promote hair follicle regeneration and wound healing.

Acknowledgements

This work was funded by the Zhejiang Province Basic Public Welfare Research Program (LGD19H110002) and Zhejiang Medical and Health Science and Technology Plan Project (2018KY832).

Disclosure of conflict of interest

None.

Address correspondence to: Ying Xia, Medical Cosmetology Department, Plastic Surgery, Shaoxing People's Hospital (Shaoxing Hospital, Zhejiang University School of Medicine), Shaoxing 312000, Zhejiang Province, P. R. China. Tel: +86-186-5758-3166; E-mail: docxiaying001@163.com; Jianshe Chen, Department of Dermatology, The First Affiliated Hospital, Xiamen University, Xiamen 361000, Fujian Province, P. R. China. E-mail: cjc09897@hotmail.com

References

[1] Zhou X, Liang L, Zhao Y and Zhang H. Epigallocatechin-3-gallate ameliorates angiotensin II-induced oxidative stress and apoptosis in human umbilical vein endothelial cells through the activation of Nrf2/Caspase-3 signaling. J Vasc Res 2017; 54: 299-308.

[2] Kim KH, Blasco-Morente G, Cuende N and Arias-Santiago S. Mesenchymal stromal cells: properties and role in management of cutaneous diseases. J Eur Acad Dermatol Venereol 2017; 31: 414-423.

[3] Jiang D, Singh K, Muschhammer J, Schatz S, Sindrilaru A, Makrantonaki E, Qi Y, Wlaschek M and Scharffetter-Kochanek K. MSCs rescue impaired wound healing in a murine LAD1 model by adaptive responses to low TGF-beta1 levels. EMBO Rep 2020; 21: e49115.

[4] Garcin CL, Ansell DM, Headon DJ, Paus R and Hardman MJ. Hair follicle bulge stem cells appear dispensable for the acute phase of wound re-epithelialization. Stem Cells 2016; 34: 1377-1385.

[5] Wang X, Wang X, Liu J, Cai T, Guo L, Wang S, Wang J, Cao Y, Ge J, Jiang Y, Tredget EE, Cao M and Wu Y. Hair follicle and sebaceous gland de novo regeneration with cultured epidermal stem cells and skin-derived precursors. Stem Cells Transl Med 2016; 5: 1695-1706.

[6] Motegi SI and Ishikawa O. Mesenchymal stem cells: the roles and functions in cutaneous wound healing and tumor growth. J Dermatol Sci 2017; 86: 83-89.

[7] Magne B, Dedier M, Nivet M, Coulomb B, Banzet S, Lataillade JJ and Trouillas M. IL-1beta-primed mesenchymal stromal cells improve epidermal substitute engraftment and wound healing via matrix metalloproteinases and transforming growth factor-beta1. J Invest Dermatol 2020; 140: 688-698, e621.

[8] Aguirre GA, Gonzalez-Guerra JL, Espinosa L and Castilla-Cortazar I. Insulin-like growth factor 1 in the cardiovascular system. Rev Physiol Biochem Pharmacol 2018; 175: 1-45.

[9] Blakytny R, Jude EB, Martin Gibson J, Boulton AJ and Ferguson MW. Lack of insulin-like growth factor 1 (IGF1) in the basal keratinocyte layer of diabetic skin and diabetic foot ulcers. J Pathol 2000; 190: 589-594.

[10] Talebpour Amiri F, Fadaei Fathabadi F, Mahmoudi Rad M, Piryae A, Ghasemi A,

Khalilian A, Yeganeh F and Mosaffa N. The effects of insulin-like growth factor-1 gene therapy and cell transplantation on rat acute wound model. Iran Red Crescent Med J 2014; 16: e16323.
[11] Rao Y, Cui J, Yin L, Liu W, Liu W, Sun M, Yan X, Wang L and Chen F. Preclinical study of mouse pluripotent parthenogenetic embryonic stem cell derivatives for the construction of tissue-engineered skin equivalent. Stem Cell Res Ther 2016; 7: 156.
[12] Castela M, Linay F, Roy E, Moguelet P, Xu J, Holzenberger M, Khosrotehrani K and Aractingi S. Igf1r signalling acts on the anagen-to-catagen transition in the hair cycle. Exp Dermatol 2017; 26: 785-791.
[13] Fu F, Qin Z, Xu C, Chen XY, Li RX, Wang LN, Peng DW, Sun HT, Tu Y, Chen C, Zhang S, Zhao ML and Li XH. Magnetic resonance imaging-three-dimensional printing technology fabricates customized scaffolds for brain tissue engineering. Neural Regen Res 2017; 12: 614-622.
[14] Tong C, Hao H, Xia L, Liu J, Ti D, Dong L, Hou Q, Song H, Liu H, Zhao Y, Fu X and Han W. Hypoxia pretreatment of bone marrow-derived mesenchymal stem cells seeded in a collagen-chitosan sponge scaffold promotes skin wound healing in diabetic rats with hindlimb ischemia. Wound Repair Regen 2016; 24: 45-56.
[15] Alapure BV, Lu Y, He M, Chu CC, Peng H, Muhale F, Brewerton YL, Bunnell B and Hong S. Accelerate healing of severe burn wounds by mouse bone marrow mesenchymal stem cell-seeded biodegradable hydrogel scaffold synthesized from arginine-based poly (ester amide) and chitosan. Stem Cells Dev 2018; 27: 1605-1620.
[16] Xia Y, You XE, Chen H, Yan YJ, He YC and Ding SZ. Epidermal growth factor promotes mesenchymal stem cell-mediated wound healing and hair follicle regeneration. Int J Clin Exp Pathol 2017; 10: 7390-7400.
[17] Kosol W, Kumar S, Marrero-Berrlos I and Berthiaume F. Medium conditioned by human mesenchymal stromal cells reverses low serum and hypoxia-induced inhibition of wound closure. Biochem Biophys Res Commun 2020; 522: 335-341.
[18] Zhang M, Liu J, Li M, Zhang S, Lu Y, Liang Y, Zhao K and Li Y. Insulin-like growth factor 1/insulin-like growth factor 1 receptor signaling protects against cell apoptosis through the PI3K/AKT pathway in glioblastoma cells. Exp Ther Med 2018; 16: 1477-1482.
[19] Zhao P, Xiao L, Peng J, Qian YQ and Huang CC. Exosomes derived from bone marrow mesenchymal stem cells improve osteoporosis through promoting osteoblast proliferation via MAPK pathway. Eur Rev Med Pharmacol Sci 2018; 22: 3962-3970.
[20] Asakawa K, Toyoshima KE and Tsuji T. Functional hair follicle regeneration by the rearrangement of stem cells. Methods Mol Biol 2017; 1597: 117-134.
[21] Li X, Ma M, Ahn DU and Huang X. Preparation and characterization of novel eggshell membrane-chitosan blend films for potential wound-care dressing: from waste to medicinal products. Int J Biol Macromol 2019; 123: 477-484.
[22] Castro NJ, Tan WN, Shen C and Zhang LG. Simulated body fluid nucleation of three-dimensional printed elastomeric scaffolds for enhanced osteogenesis. Tissue Eng Part A 2016; 22: 940-948.
[23] Herrmann M, Hildebrand M, Menzel U, Fahy N, Alini M, Lang S, Benneker L, Verrier S, Stoddart MJ and Bara JJ. Phenotypic characterization of bone marrow mononuclear cells and derived stromal cell populations from human iliac crest, vertebral body and femoral head. Int J Mol Sci 2019; 20: 3454.
[24] An Y, Liu WJ, Xue P, Ma Y, Zhang LQ, Zhu B, Qi M, Li LY, Zhang YJ, Wang QT and Jin Y. Autophagy promotes MSC-mediated vascularization in cutaneous wound healing via regulation of VEGF secretion. Cell Death Dis 2018; 9: 58.
[25] An R, Zhang Y, Qiao Y, Song L, Wang H and Dong X. Adipose stem cells isolated from diabetic mice improve cutaneous wound healing in streptozotocin-induced diabetic mice. Stem Cell Res Ther 2020; 11: 120.
[26] Qi C, Xu L, Deng Y, Wang G, Wang Z and Wang L. Sericin hydrogels promote skin wound healing with effective regeneration of hair follicles and sebaceous glands after complete loss of epidermis and dermis. Biomater Sci 2018; 6: 2859-2870.
[27] Vijayan A, A S and Kumar GSV. PEG grafted chitosan scaffold for dual growth factor delivery for enhanced wound healing. Sci Rep 2019; 9: 19165.
[28] Wang S, Mo M, Wang J, Sadia S, Shi B, Fu X, Yu L, Tredget EE and Wu Y. Platelet-derived growth factor receptor beta identifies mesenchymal stem cells with enhanced engraftment to tissue injury and pro-angiogenic property. Cell Mol Life Sci 2018; 75: 547-561.
[29] Zhang X, Kang X, Jin L, Bai J, Liu W and Wang Z. Stimulation of wound healing using bioinspired hydrogels with basic fibroblast growth factor (bFGF). Int J Nanomedicine 2018; 13: 3897-3906.
[30] Mukai K, Tsai M, Saito H and Galli SJ. Mast cells as sources of cytokines, chemokines, and growth factors. Immunol Rev 2018; 282: 121-150.

[31] Han N, Jia L, Guo L, Su Y, Luo Z, Du J, Mei S and Liu Y. Balanced oral pathogenic bacteria and probiotics promoted wound healing via maintaining mesenchymal stem cell homeostasis. Stem Cell Res Ther 2020; 11: 61.
[32] Hakuno F and Takahashi SI. IGF1 receptor signaling pathways. J Mol Endocrinol 2018; 61: T69-T86.
[33] Lin M, Liu X, Zheng H, Huang X, Wu Y, Huang A, Zhu H, Hu Y, Mai W and Huang Y. IGF-1 enhances BMSC viability, migration, and anti-apoptosis in myocardial infarction via secreted frizzled-related protein 2 pathway. Stem Cell Res Ther 2020; 11: 22.
[34] Stuard WL, Titone R and Robertson DM. The IGF/insulin-IGFBP axis in corneal development, wound healing, and disease. Front Endocrinol (Lausanne) 2020; 11: 24.
[35] Wahedi HM, Jeong M, Chae JK, Do SG, Yoon H and Kim SY. Aloesin from Aloe vera accelerates skin wound healing by modulating MAPK/Rho and Smad signaling pathways in vitro and in vivo. Phytomedicine 2017; 28: 19-26.
[36] Sbaraglini ML, Molinuevo MS, Sedlinsky C, Schurman L and McCarthy AD. Saxagliptin affects long-bone microarchitecture and decreases the osteogenic potential of bone marrow stromal cells. Eur J Pharmacol 2014; 727: 8-14.
[37] Dhoke NR, Kaushik K and Das A. Cxcr6-based mesenchymal stem cell gene therapy potentiates skin regeneration in murine diabetic wounds. Mol Ther 2020; 28: 1314-1326.